J. Chem. Sci. Vol. 126, No. 4, July 2014, pp. 1217–1226.

Ab initio study of solvent-dependent one-, two- and three-photon absorption properties of PRODAN-based chemo-sensors

MD MEHBOOB ALAM* and MAUSUMI CHATTOPADHYAYA
Department of Chemistry, University of Calcutta, Kolkata 700 009, West Bengal, India
e-mail: mehboob.cu@gmail.com

MS received 25 September 2013; revised 21 February 2014; accepted 22 March 2014

Abstract. In this work, we study the solvent-dependent one-, two- and three-photon absorption (1PA, 2PA and 3PA) properties of 2-propionyl-6-dimethylamino naphthalene (PRODAN) and three newly synthesized[20] cyclopenta[b]naphthalene derivatives, in gas phase and three different solvents, namely cyclohexane, dichloromethane and ethanol. A comparison between the calculated and the available experimental data shows that the results obtained with B3LYP/cc-pVDZ level of theory matches well with the experimental absorption data for all of these compounds. The 2P and 3P transition probabilities, for all of these systems, are found to be maximum in solvents of intermediate polarity (here, dichloromethane), which is in accordance with the experimental observation for various other systems. All the 1P, 2P and 3P transition probabilities are found to be the maximum for PRODAN as compared to other three molecules in both the gas as well as the different solvent phases (except for 3PA in gas and cyclohexane solvents). We have explained these results by meticulously inspecting the components of different transition moment vectors and the tensor elements involved.

Keywords. Response theory; TDDFT; solvent effect; computational chemistry; non-linear optical property.

1. Introduction

6-Propionyl-2-(*N*, *N*-dimethylamino)naphthalene (PRODAN)[1–3] is a naphthalene-based organic molecule having tertiary amine as a donor and acyl as an acceptor group. It is well known for its fluorescent property and serves as a chemo-sensor of micropolarity. Its huge popularity is because of its smaller size, which decreases its interaction with the environment and also the response time during event-monitoring. At the same time, since the donor and acceptor groups in this molecule are placed at the maximum distance apart, a large difference in dipole moment between the ground and excited states is observed during charge transfer from donor to acceptor moieties. This causes a remarkable solvatochromic effects in fluorescence spectra of this system.[4,5] It was first prepared by Weber *et al.*[1] for probing the binding site of albumin but, later on, this molecule along with its various derivatives has extensively been used as fluorescence probe for monitoring microenvironments in different biological and chemical reactions.[6–8] At the same time, it has also found applications in other fields of research such as interactions of alcohol with biological membranes,[9] solute effects on phase transitions,[10] water content in reverse micelles,[11] oxidative damage of phospholipids,[12] interfacial properties of ether lipids,[13,14] surface properties of cholesterol-membrane,[15,16] fluidity of lipid mixtures[17] and many more to mention.[18,19] Such an extensive list of applications has led the researchers to find various derivatives of PRODAN, which can be made more and more useful. In this direction, recently, Benedetti *et al.*[20] have synthesized a series of PRODAN-based solvatochromic fluorophores and studied their absorption and emission spectra in different solvents. In their work[20] they have found that most of the fluorophores have high quantum yield and large Stokes shifts in CH_2Cl_2 solvent. In addition to the aforementioned studies, several experimental and theoretical works have also been devoted to study the photo-physical behavior of PRODAN and related compounds. In 2003, Lobo *et al.*[21] based on their experimental studies, have concluded that emission in PRODAN occurs from a planar intramolecular charge transfer state. This observation was verified in 2005 by Davis and Abelt.[22] Similarly, in 2007, Mennucci *et al.*[23] from their quantum chemical study of electronic properties of PRODAN in both the homogeneous and heterogeneous environments, have concluded that in both the polar and apolar solvents, emission occurs from a planar S_1 state. In the same year, Novaira *et al.*[24] have studied the photo-physical behavior of PRODAN in anionic and cationic reverse

*For correspondence

micelles. Similar conclusion is also drawn by Adhikary *et al.*[25] in their solvation dynamics study of PRODAN in heterogeneous environments. In 2010, Everett *et al.*[26] have concluded that the intramolecular charge-transfer excited state of PRODAN is planar. They have further found that in protic solvents, twisting about the carbonyl group quenches the excited state. Recently, Cwiklik *et al.*[27] have studied the absorption and fluorescence spectra of PRODAN in phospholipid bilayers using both the experimental and the theoretical QM/MD techniques and have concluded that in cyclohexane the $S_1 \rightarrow S_0$ transition occurs from planar S_1 state, whereas in water and in phospholipid bilayer, emission can occur from both the twisted and planar states. From this literature survey it is clear that most of the studies of PRODAN are related to the nature and structure of the excited state from where emission occurs, but till now, no work has been done for studying the non-linear optical properties of this system. In the present work, we have studied the one-, two- and three-photon absorption (1PA, 2PA and 3PA) properties of PRODAN and three of its newly synthesized derivatives in gas phase as well as in three different solvents of varying polarity, namely cyclohexane (C_6H_{12}), dichloromethane (CH_2Cl_2) and ethanol (C_2H_5OH). The reason for choosing these solvents is simply their polarity and we expect it to be appropriate for studying the solvent effect on the properties considered. It is important to mention here that the particular choice of CH_2Cl_2 solvent is that, in their work, Benedetti *et al.*[20] have shown that PRODAN and the other three molecules (considered in this work) have shown maximum quantum yield in this solvent. We have employed the linear, quadratic, and cubic response theories[28–32] as well as two-state model (2SM)[33,34] approach to explain the 1P, 2P and 3P transition probabilities of all these systems.

2. Methods and calculations

Ground-state geometries of all the systems studied in this work have been optimized at the B3LYP/6-311++G (d, p) level of theory. For solvent-phase geometry optimizations, polarizable continuum model (PCM),[35] as implemented in Gaussian 09 package,[36] has been used. In order to check the reliability of the optimized geometries, we have performed vibrational frequency analysis at the same level of theory. The absence of any imaginary frequency ascertains that the optimized geometries belong to minima on the respective potential energy surfaces. After the ground-state geometry optimizations and frequency calculations, we have employed the linear, quadratic and cubic response theories to calculate the 1P, 2P and 3P transition parameters of all these systems in gas and three different solvent phases. For this purpose we have employed the TDDFT method using B3LYP functional and cc-pVDZ basis set, and for the solvent phase calculations, the non-equilibrium formulation[37,38] of TDDFT within PCM as implemented in DALTON[39] program package have been used. The justification for using the B3LYP/cc-pVDZ level of theory is discussed in section 3. Here it is important to mention that, considering the huge computational cost for the cubic response 3PA calculations, we have performed this for the first two systems and only in gas phase. Finally, we have employed the 2SM approach for re-evaluating the 2P and 3P transition probabilities of all the systems in gas and different solvent phases. Different quantities required for the 2SM calculations have also been calculated at the B3LYP/cc-pVDZ level of theory of DALTON software package. All these calculations have been done at a workstation having AMD FX(tm)-8350 Eight-Core processor (4.00 GHz) and 32 GB RAM. Each optimization, on an average, took ~4–6 hours to complete. Each gas-phase linear response 1PA calculations for two roots in DALTON code consumed ~60–120 hours, depending on the size of the systems and the medium used (gas phase or solvent phase). Similarly, the quadratic response 2PA consumed ~90–200 hours and cubic response 3PA calculations for only one root and only in gas phase took ~30 hours to complete. These details clearly indicate that response theory calculations are very much expensive.

3. Results and discussion

Let us first discuss the ground-state geometries of the four systems studied in this work. The systems chosen for this study have been labeled as A, B, C and D (where D is PRODAN) and the gas phase-optimized structures of all the systems have been depicted in figure 1. (The optimized Cartesian co-ordinates of all the systems in both the gas and the solvent phases have been supplied in supplementary information). All the four systems have, in common, a naphthalene ring and the donor group -NMe_2. In A, B and C molecules, -$COCH_3$ is the acceptor group, whereas D has -COC_2H_5 as the acceptor moiety. Except in D, all the other three molecules have a five-member ring fused with the naphthalene ring on the acceptor side. The optimized geometries in figure 1 clearly indicate that all the four molecules lie in *xy*-plane and the donor–acceptor groups lie approximately along the *x*-axis. Similar orientations for all the

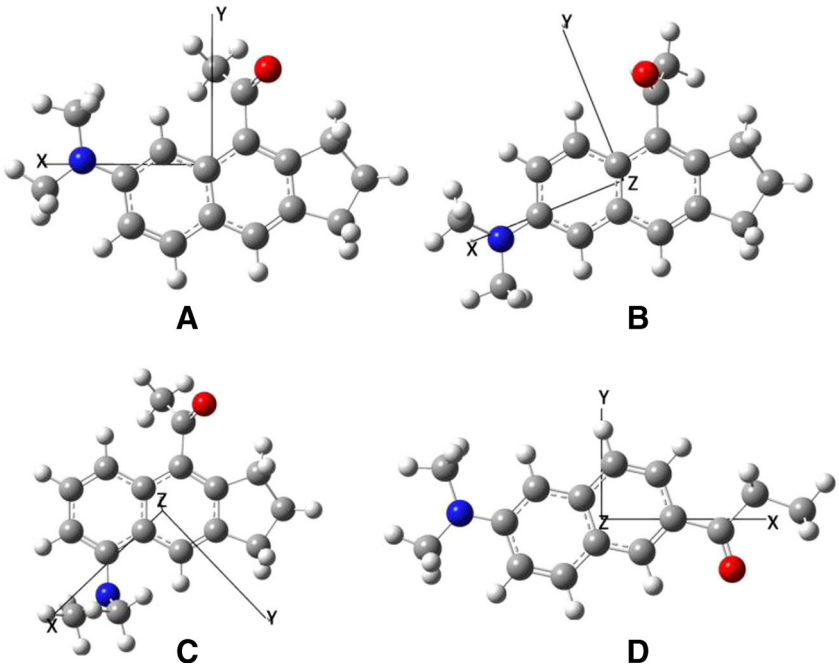

Figure 1. Gas phase-optimized geometries of four molecules (A, B, C and D) studied in this work.

molecules are also obtained in different solvent phases. A close scrutiny of the geometries of all these systems in gas and different solvent phases indicates that no significant geometrical changes occur on moving from either gas phase to solvent phase or from one solvent to another.

3.1 *Choosing appropriate density functional method/basis-set combination*

Following the geometrical description let us move on to find an appropriate density functional method and basis set for the calculation of concerned properties. To do so, we have evaluated the excitation energy for the ground to first excited-state transition of molecule A in cyclohexane solvent using four well-known density functional methods (viz. PBE (Perdew, Becke, Ernzerhof), VWN (Vosko, Wilk, Nusair), B3LYP (Becke-3-parameters Lee, Yang, Parr) and CAMB3LYP (Coulomb attenuated method - Becke-3-parameters Lee Yang Parr)) and five different basis sets (viz. 6-31+G (d), 6-311+G (d), 6-311++G (d, p), cc-pVDZ and aug-cc-pVDZ) and compare the results with the experimentally available data. Of course, various other density functional methods and basis sets are available, but we think those considered here are sufficient for analysis. It is also important to mention here that, for this analysis, there is no specific reason for choosing molecule A in cyclohexane solvent as the experimental data are also available for all the four molecules in various other solvents. The results of this analysis are presented in table 1. The experimental excitation energy (in terms of wavelength) for molecule A in cyclohexane solvent is 373 nm.[20] It is obvious from the results in table 1 that irrespective of the basis sets used, the B3LYP, PBE and VWN methods overestimate the experimental excitation energy, whereas CAMB3LYP underestimates it. Out of these 20 different combinations of density functional methods and basis sets, we have found that the result obtained with the B3LYP/cc-pVDZ level of theory is the one that is the closest to the experimental value. In this case, the difference between B3LYP/cc-pVDZ result and the experimental value is only 14.61 nm. On the basis of this analysis, we have concluded that the B3LYP/cc-pVDZ level of theory is appropriate for this study and hence we decided to carry out the rest of the calculations at this level of theory. In this case, although the DFT method gives experimentally closer results, it is important to mention that these methods have their own limitations, particularly in case of excited state calculations. In many cases it reverses the energy ordering of the two states as predicted by other wave function-based methods. One such example is the energy ordering of S_1 and S_2 states of hexafluorobenzene.[40–42] It is also important to mention here that the electronic non-adiabatic effects[43–45] may play a vital role in the excited state properties of the studied systems. But as these effects cannot be studied using the available TDDFT methods in DALTON code, we have not included this effect in the present work. However, needless to say, such effects definitely can highlight new fealtures of the properties studied in this work.

Table 1. 1PA excitation energies (in nm) of molecule A in cyclohexane solvent, obtained with different combinations of density functional methods and basis sets.

Functional → Basis set ↓	PBE	VWN	B3LYP	CAMB3LYP	Experimental
6-31+G(d)	485.87	497.82	396.17	337.43	373
6-311+G(d)	485.04	498.13	397.23	339.10	
6-311++G(d,p)	485.58	498.92	397.84	339.73	
cc-pVDZ	471.63	482.74	387.61	333.69	
aug-cc-pVDZ	487.33	499.05	398.41	340.96	

3.2 *One-photon absorption process*

1PA is defined as the excitation from one electronic state to another by the absorption of a single photon of incident radiation. It is characterized by the wavelength corresponding to the maximum in the absorption spectrum and can be studied using linear response theory. The 1PA results for all the systems in gas phase as well as in different solvent phases (cyclohexane, CH_2Cl_2 and C_2H_5OH), calculated at the B3LYP/cc-pVDZ level of theory are presented in table 2. It is important to mention here that no gas phase experimental data are available for any of these molecules. A comparison of calculated 1PA wavelengths of molecule A in cyclohexane, CH_2Cl_2 and C_2H_5OH solvents (385.43, 391.05 and 391.22 nm) with the experimental[20] values (373, 377 and 377 nm) reveals a nice agreement between the two. For D, the calculated (and experimental) results in CH_2Cl_2 and C_2H_5OH solvents are 355 (367.98) and 362 (364.93) nm, respectively. Similarly, for B and C molecules, the calculated values are very close to the experimental results (table 2). These results further verify the correctness of the density functional method/basis set used. It is necessary to mention here that the minimum difference between theoretical and experimental results is 2.43 nm (which is for molecule D in C_2H_5OH solvent) and the corresponding maximum difference is 39.55 nm for molecule C in cyclohexane solvent. Our theoretical results predict that, for all of these systems, the value of 1PA wavelength increases very slowly with the increase in solvent polarity and is consistent with the experimental observation, as evident from the data in table 2.

The strength of 1PA process in a system is measured in terms of oscillator strength and for a transition from ground state |0> to final state |*f*> it is given by the expression[46,47]

$$\delta_{1PA} = \frac{2\omega_f}{3}\sum_{\alpha}\left|\langle 0|\,\hat{\mu}_\alpha\,|f\rangle\right|^2 = \frac{2\omega_f}{3}\sum_{\alpha}\left|\hat{\mu}_\alpha^{0f}\right|^2 \quad (1)$$

Table 2. Polarity (ε) of the solvent, excitation energies (ω_1 in eV), theoretical ($\lambda^{calc.}$ in nm) and experimental ($\lambda^{Expt.}$ in nm) 1PA wavelength, oscillator strength (δ_{1PA} in a.u.), transition dipole moment (μ^{01} in a.u.), difference between ground- and excited-state dipole moment ($\Delta\mu^{11}$ in a.u.) for ground- to first excited-state transition in gas as well as in different solvent phases of all the four molecules. NA is acronym for "not available."

System	Solvent	ε of solvent	ω_1 (eV)	λ^{Theo}, λ^{Expt} (nm)	δ_{1PA} (a.u.)	μ^{01} (a.u.)	$\Delta\mu^{11}$ (a.u.)	Λ	Orbitals
A	Gas		3.29	376.93, NA	0.10	1.24	2.35	0.64	H-L (−0.69)
	cyclohexane	2.023	3.22	385.19, 373	0.12	1.39	2.68	0.63	H-L (−0.69)
	CH_2Cl_2	8.930	3.17	391.05, 377	0.12	1.38	2.75	0.62	H-L (−0.70)
	C_2H_5OH	24.550	3.16	391.92, 377	0.12	1.35	2.74	0.62	H-L (−0.70)
B	Gas		3.52	352.39, NA	0.05	0.91	2.63	0.68	H-L (0.69)
	cyclohexane	2.023	3.47	357.02, 363	0.06	1.03	2.98	0.68	H-L (0.69)
	CH_2Cl_2	8.930	3.42	362.95, 372	0.06	1.01	3.20	0.66	H-L (−0.69)
	C_2H_5OH	24.550	3.40	364.62, 374	0.06	0.99	3.24	0.65	H-L (−0.69)
C	Gas		3.43	361.24, NA	0.08	1.04	3.14	0.65	H-L (0.69)
	cyclohexane	2.023	3.51	353.55, 314	0.09	1.12	3.35	0.66	H-L (−0.69)
	CH_2Cl_2	8.930	3.49	355.69, 334	0.09	1.10	3.44	0.65	H-L (−0.69)
	C_2H_5OH	24.550	3.48	355.93, 334	0.09	1.09	3.43	0.65	H-L (−0.69)
D	Gas		3.54	350.54, NA	0.25	1.74	2.29	0.70	H-L (−0.67)
	cyclohexane	2.023	3.44	360.30, NA	0.35	2.09	2.73	0.69	H-L (0.69)
	CH_2Cl_2	8.930	3.37	367.98, 355	0.38	2.19	2.80	0.67	H-L (−0.69)
	C_2H_5OH	24.550	3.36	369.43, 362	0.38	2.18	2.77	0.67	H-L (−0.69)

Here, the summation is taken over all the coordinate axes x, y, and z. ω_f and μ^{0f} are, respectively, the excitation energy and the transition dipole moment vector for the said transition. The larger the value of these two quantities the larger will be the oscillator strength. Results in table 2 clearly indicate that the oscillator strengths for A, B and C molecules are very small as compared to that of D and follows the order A > C > B. The reason for this order and the relatively larger value for D becomes clear from equation 1 and the results in table 2. The excitation energy for D is slightly larger than the other three molecules, whereas its μ^{0f} is much larger than the others. Therefore, the quadratic dependence of oscillator strength on μ^{0f} makes it much larger for D as compared to the other three molecules. Similarly, the order of oscillator strength for the other three molecules, i.e., A > C > B, is because of the stronger impact of μ^{0f} than ω_f on δ_{1PA}. It is also important to note that the value of δ_{1PA} for D gradually increases with the increase in solvent polarity and very soon it gets saturated. This molecule (D) has almost the same value for δ_{1PA} in both the CH_2Cl_2 and C_2H_5OH solvents. For the other three molecules, δ_{1PA} has more or less the same value in different solvents. It happens because of the smaller magnitude and no or very little solvent effect on μ^{0f} and ω_f of these systems.

3.3 *Orbital analysis and nature of $S_1 \leftarrow S_0$ transition*

In order to analyze the short-/long-range nature of the transition considered in this work and the role of different orbital transitions in the same we have calculated the contributions of different orbital transitions involved in the first transition ($S_1 \leftarrow S_0$) of all the four molecules in both the gas and in different solvent phases. The relevant data are supplied in table 2. The results clearly indicate that irrespective of the nature of solvents used, the only major contributing orbitals pair involved in $S_1 \leftarrow S_0$ transition in all these molecules is HOMO-LUMO, which shares more than 60% of contribution. The orbital pictures for all the molecules in gas phase are supplied in figure 2. We did not show the solvent-phase orbital pictures here, as these are identical to those in the gas phase. The orbital pictures clearly indicate that neither HOMO nor LUMO for any of these molecules is concentrated to any specific part, rather these are spread throughout the molecules, which reveals that HOMO-LUMO transition is essentially a local, short-range $\pi - \pi^*$ type of transition. In order to confirm this result, we have further calculated the discriminator for short-/long-range nature of transition, which is popularly known as Λ parameter.[48] Its values lie between 0 and 1. Large values of Λ indicate a significant overlap between the virtual and occupied orbitals involved, and hence its large value essentially characterizes a short-range nature of transition. It is used by several authors for determining the nature of transitions in various types of molecules.[34,49–54] The values of Λ parameters for all the systems in both the gas and solvent phases are also listed in table 2. Results show that the value of Λ for the four molecules lies in between 0.62 and 0.70, which is essentially a large value and hence the $S_1 \leftarrow S_0$ transition in all these molecules is a short-range type of transition, which validates the conclusion of orbital analysis.

3.4 *Two-photon absorption process*

2PA is defined as the excitation from one electronic state to another by the synchronized absorption of two photons of same or different energies.[55–64] It is characterized by the two-photon transition probability (δ_{2P}), which, for a linearly polarized single beam of monochromatic light, is given (in a.u.) by the equation[65]

$$\begin{aligned}\delta_{2P} &= 6\left(S_{xx}^2 + S_{yy}^2 + S_{zz}^2\right) + 8\left(S_{xy}^2 + S_{xz}^2 + S_{yz}^2\right) \\ &\quad +4\left(S_{xx}S_{yy} + S_{xx}S_{zz} + S_{yy}S_{zz}\right) \qquad (2)\end{aligned}$$

Where $S_{\alpha\beta}$ terms are called two-photon tensor elements and are given by[65]

$$\begin{aligned}S_{\alpha\beta} &= \sum_i \left[\frac{\langle 0|\hat{\mu}_\alpha|i\rangle\langle i|\hat{\mu}_\beta|f\rangle}{\omega_i - \frac{\omega_f}{2}} + \frac{\langle 0|\hat{\mu}_\beta|i\rangle\langle i|\hat{\mu}_\alpha|f\rangle}{\omega_i - \frac{\omega_f}{2}}\right] \\ &= \sum_i \frac{\hat{\mu}_\alpha^{0i}\hat{\mu}_\beta^{if} + \hat{\mu}_\beta^{0i}\hat{\mu}_\alpha^{if}}{\omega_i - \frac{\omega_f}{2}} \qquad (3)\end{aligned}$$

Here α and β represent the Cartesian axes (x, y, z) and the summation runs over all the intermediate states (i). $\hat{\mu}_\alpha$ represents the α^{th} component of dipole moment operator, f is the final excited state and ω terms represent the excitation energies for excitation from ground to the respective excited states. The response theory results for all the 2P tensor elements and overall δ_{2P} of all the systems in gas and different solvent phases are supplied in tables 3 and 4. Results in table 3 clearly show that among the six different $S_{\alpha\beta}$ terms, irrespective of the nature of the solvents, only S_{xx} is highly contributing to all the systems. Moreover, S_{yy} (except C) and S_{xy} also have a small contribution. All the other components have negligibly small values for these molecules in both the gas and different solvent phases. It is important to note here that the dominance of these specific components is closely related to the orientation of the molecules in the xy plane. All the components

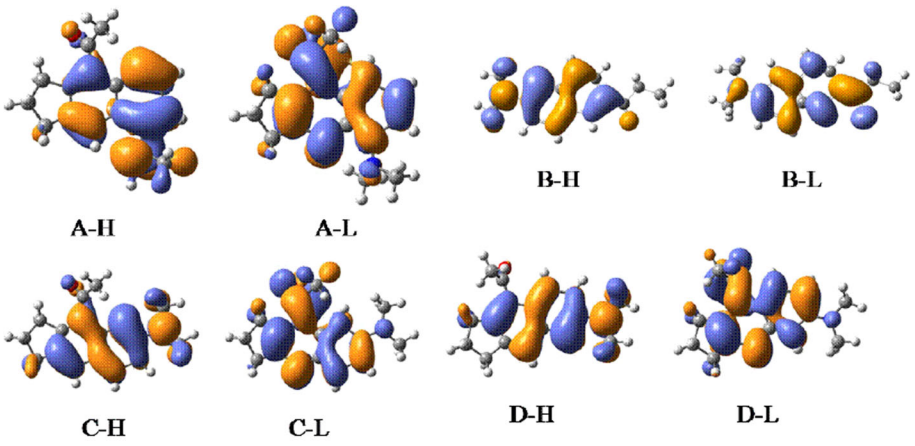

Figure 2. Orbital pictures: A-H, B-H, C-H and D-H are HOMOs of A, B, C and D molecules, respectively, whereas A-L, B-L, C-L and D-L are their LUMOs. The orientation of the molecules is the same as shown in figure 1.

having z-contribution (S_{zz}, S_{xz} and S_{yz}), i.e., perpendicular to the molecular plane, are apparently non-contributing to the overall δ_{2P} values. As shown in figure 1, all the molecules are oriented in such a way that the donor–acceptor groups lie along the x-axis. Therefore, the maximum value of S_{xx} component reflects the charge transfer between the donor–acceptor pair of the molecules. It is also very interesting to note that the orbital transition for $S_1 \leftarrow S_0$ transition is also in the x-direction, i.e., from the donor to acceptor groups in all the four molecules, which explains the dominance of S_{xx} tensor elements. We have also noted that the value of S_{xx} in different solvent phases is always greater than its value in gas phase for all the systems and is found to be the maximum in solvent of intermediate polarity (here, CH_2Cl_2). It is no surprise that the overall δ_{2P} values also follow the same trend for all these systems. Among the four systems, the last one (i.e., PRODAN, D) is found to have the highest value of δ_{2P} in gas phase as well as in different solvents, whereas molecule B has the least. For D the highest value of δ_{2P} is found to be 2.44×10^5 a.u., whereas that for B is found to be 2.82×10^4 a.u., about ten times less. In order to explain the highest 2P activity of D over the other molecules, the highest δ_{2P} value in CH_2Cl_2 solvent and the dominant contribution of S_{xx} component, we have employed the few-state model-based 2SM approach. In 2SM, the summation in equation 3 runs over $i = 0$ and f only (i.e.,

Table 3. Response theory results for 2P tensor elements (in a.u.) of all the systems in gas and different solvent phases (calculated at the B3LYP/cc-pVDZ level of theory).

Systems	Solvents	2P tensor elements (in a.u.)					
		S_{xx}	S_{yy}	S_{zz}	S_{xy}	S_{xz}	S_{yz}
A	Gas	71.9	10.8	−0.4	−21.7	−2.0	1.5
	cyclohexane	−92.6	−14.5	0.5	27.8	2.3	−1.8
	CH_2Cl_2	94.2	15.7	−0.5	−28.9	−2.3	1.7
	C_2H_5OH	−92.0	−15.7	0.5	28.4	2.1	−1.6
B	Gas	53.0	−9.0	−0.4	14.7	1.3	−0.1
	cyclohexane	66.9	−11.4	−0.4	18.8	1.6	−0.1
	CH_2Cl_2	67.9	−13.3	−0.4	19.9	1.7	−0.1
	C_2H_5OH	66.5	−13.6	−0.3	19.8	1.6	−0.1
C	Gas	59.6	0.4	−0.5	20.1	0.3	0.5
	cyclohexane	61.8	0.1	−0.7	22.1	−0.1	0.3
	CH_2Cl_2	62.0	0.1	−0.7	22.3	−0.2	0.2
	C_2H_5OH	−60.6	−0.2	0.7	−21.8	0.2	−0.2
D	Gas	138.4	−8.7	−1.0	−7.2	−0.2	−0.1
	cyclohexane	191.5	−11.2	−1.1	−11.0	−0.3	0.0
	CH_2Cl_2	−204.9	11.3	1.0	13.1	−0.4	0.0
	C_2H_5OH	−202.6	11.1	1.0	13.2	0.4	0.0

Table 4. Components of μ^{0f} and $\Delta\mu^{ff}$ vectors, response and 2SM results for δ_{2P} values (in a.u.) of all the systems in gas and different solvent phases (calculated at the B3LYP/cc-pVDZ level of theory).

System	Solvent	Component of μ^{0f} (a.u.)			Component of $\Delta\mu^{ff}$ (a.u.)			δ_{2P} (Resp.)	δ_{2P} (2SM)	$\theta°$
		x	y	z	x	y	z			
A	Gas	−1.056	0.641	0.001	−2.286	0.540	0.111	38.40	51.94	161.9
	Cyclohexane	−1.201	0.709	0.005	−2.589	0.664	0.114	64.20	90.44	163.7
	CH_2Cl_2	−1.190	0.696	0.006	−2.640	0.749	0.110	67.20	97.06	165.4
	C_2H_5OH	−1.167	0.683	0.006	−2.623	0.767	0.107	64.20	93.36	165.8
B	Gas	−0.634	0.653	0.005	−2.566	0.576	−0.007	17.10	16.96	121.6
	Cyclohexane	−0.729	−0.734	−0.006	−2.899	0.672	−0.010	27.39	28.92	122.7
	CH_2Cl_2	0.706	0.720	0.008	−3.092	0.829	−0.010	28.20	31.37	119.5
	C_2H_5OH	0.686	0.706	0.009	−3.122	0.872	−0.010	27.09	30.45	118.6
C	Gas	−0.951	−0.413	0.005	−3.129	−0.271	−0.070	24.48	59.71	161.4
	Cyclohexane	−1.023	−0.459	0.002	−3.338	−0.258	−0.059	26.70	75.23	160.2
	CH_2Cl_2	−1.008	−0.450	0.0	−3.423	−0.291	−0.054	26.88	78.08	160.8
	C_2H_5OH	−0.992	−0.442	0.0	−3.412	−0.299	−0.053	25.74	75.37	160.1
D	Gas	−1.690	−0.423	0.023	2.233	−0.487	−0.016	110.40	78.22	153.7
	Cyclohexane	−2.044	−0.433	0.024	2.672	−0.561	−0.014	212.40	174.14	156.2
	CH_2Cl_2	2.149	0.399	−0.020	2.739	−0.579	−0.011	244.20	211.54	157.5
	C_2H_5OH	2.145	0.387	−0.019	2.708	−0.576	−0.010	237.80	207.77	157.7

ground and the final excited states only). Therefore, after simplification, expression for $S_{\alpha\beta}$ becomes[33,34]

$$S_{\alpha\beta} = \frac{2\left(\hat{\mu}_{\alpha}^{0f}\Delta\hat{\mu}_{\beta}^{ff} + \hat{\mu}_{\beta}^{0f}\Delta\hat{\mu}_{\alpha}^{ff}\right)}{\omega_f} \tag{4}$$

In this expression, $S_{\alpha\beta}$ depends on the ground- to final excited-state transition moment, corresponding excitation energy and the dipole moment difference between the two states only. This expression is much easier to comprehend as compared to the full sum-over-states expression (equation 3) in which the involvement of all the intermediate states makes it much harder to correlate with the overall δ_{2P} value. When we put this 2SM expression of $S_{\alpha\beta}$ in equation 2 and utilize the vector nature of μ^{0f} and $\Delta\mu^{ff}$, the expression for δ_{2P} within 2SM approach becomes[33,34]

$$\delta_{2P}^{2SM} = 32\left(\frac{\mu^{0f}\Delta\mu^{ff}}{\omega_f}\right)^2\left(2\cos^2\theta + 1\right) \tag{5}$$

Here, θ represents the angle between μ^{0f} and $\Delta\mu^{ff}$ vectors. Using equations 4 and 5, the highest contributing S_{xx} tensor element and the overall δ_{2P} values for all the systems in gas and in different solvent phases have been calculated. The results from the 2SM approach and different components of μ^{0f} and $\Delta\mu^{ff}$ are presented in table 4. It is obvious from the results that the x and y components of both μ^{0f} and $\Delta\mu^{ff}$ are much larger than the corresponding z component and among the two (i.e., x and y components), the latter has always the smaller value for all the molecules (except μ^{0f} of molecule B, where both these components have comparable values), in both the gas and in different solvent phases. The larger values of x and y components again reflect the charge transfer between the donor–acceptor pair within the molecular plane of all these molecules and it causes the highest contribution of the S_{xx} tensor element. The values of the S_{xx} component for D, as obtained using the 2SM approach, in gas, cyclohexane, CH_2Cl_2 and C_2H_5OH solvents are, respectively, -116.15, -172.83, 190.17 and 188.41 a.u., which are very close to the response theory results given in table 3. Similarly, for molecules A, B and C, the values of the S_{xx} component are (79.95, -92.6, 94.2, -92.0), (-50.36, 66.24, -69.58, -68.63) and (94.41, 106.78, 107.78, 105.82) respectively. It is important to mention here that the values of overall δ_{2P}, as obtained from the 2SM approach, are also in good agreement with the response theory results. From the data in table 4 one can notice that, for molecules A, C and D, the value of θ-dependent term (i.e., $cos^2\theta$) in equation 5 is very close to its maximum value of 1 but for B its value is around 0.5. At the same time, the value of S_{xx} term is least for B due to the smallest value of x-component of μ^{0f}. All these factors in turn make the δ_{2P} for B, the smallest one. Similarly, the largest value of δ_{2P} for molecule D is because of the largest x-component of μ^{0f}. Regarding the solvent dependency, we have noticed that although both the S_{xx} component and the overall δ_{2P} values for all the systems are largest in CH_2Cl_2 solvent, the x component of neither μ^{0f} nor $\Delta\mu^{ff}$ is largest in this solvent. However, if we consider the product of the two terms (x-components of μ^{0f} and $\Delta\mu^{ff}$) we notice that this product is the maximum

in CH_2Cl_2 solvent for all the four molecules. Thus, it is clear that the largest contribution of the S_{xx} component over others is mainly because of the largest value of x-component of μ^{0f} and it also explains the highest δ_{2P} values for D and smallest for B molecules. Therefore, the maximum value of δ_{2P} for all these systems in CH_2Cl_2 solvent is due to the combined effect of μ^{0f} and $\Delta\mu^{ff}$ vectors. It is important to mention here that as the orbital nature remains more or less same in both the gas phase and different solvents, it is not possible to explain these results on the basis of orbital pictures.

3.5 *Three-photon absorption process*

3PA is characterized by the three-photon transition probability (δ_{3P}). As δ_{2P} is related to the 2P-tensor elements, δ_{3P} is similarly related to three-photon tensor elements (T_{ijk}), which can be expressed in terms of ground to excited states, excited to excited states transition moment vectors and excitation energies, by the relation[28]

$$T_{ijk} = \sum P_{ijk} \sum_{m,n} \frac{\hat{\mu}_i^{0m} \hat{\mu}_j^{mn} \hat{\mu}_k^{nf}}{\left(\omega_m - \frac{\omega_f}{3}\right)\left(\omega_n - \frac{2\omega_f}{3}\right)} \qquad (6)$$

Where i, j, k represent the Cartesian axes (x, y, z) and $\sum P_{ijk}$ represents the summation over all the permutation of the indices i, j, k. The relation between δ_{3P} and different T_{ijk} terms, for a single beam of linearly polarized monochromatic light, is given by[28]

$$\delta^{3P} = 2\sum_{i,j,k} T_{iij} T_{kkj} + 3\sum_{i,j,k} T_{ijk}^2. \qquad (7)$$

The value of δ_{3P} can be calculated using the single residue of cubic response theory, but computationally it is very expensive. Considering the huge computational cost of calculating the 3P parameters of a system, it is not wise to apply it directly on the concerned systems. Hence, we have used the alternative method (i.e., the few-state model-based 2SM approach) for calculating the 3P parameters of all the systems in both the gas and different solvent phases. As this method involves only two states (i.e., ground and the final excited states), it is computationally less expensive. However, before describing the 2SM approach and presenting the corresponding results, we must mention here that the previous studies have shown that for the 3PA process the 2SM approach is not as successful as it is for the 2PA process. The limitations and usefulness of the 2SM approach, in the case of 3PA, is well documented in the work by Cronstrand *et al*. In their work, they have pointed out that few-state model performs fine for smaller systems like LiH, but it shows convergence problem for larger systems. They have further demonstrated that for relatively smaller molecules like *p*-Nitroaniline, even after involving 15 intermediate states, the difference of T_{zzz} component obtained from the response theory and the few-state model approach is about 1.5 times and this aspect is found to be consistent for *trans*-stilbene-based larger systems. In spite of this discrepancy between the response theory and few-state model results, they have proposed that the few-state model for 3PA process may be used for the interpretation purposes. In addition to the aforementioned limitation, one must also keep in mind that the success of the few-state model approach depends on the contributions of the intermediate states involved in the calculations. For obtaining computationally good results, we must involve the highly contributing intermediate states in the calculations. Keeping these advantages and limitations in mind, the 2SM results for all the systems are presented in this work. Similar to 2PA, we have calculated only the T_{xxx} component and the overall δ_{3P} for all the systems. Within the 2SM, the value of T_{xxx} tensor element is given by the expression[66–68]

$$T_{xxx}^{2SM} = \frac{27}{2\omega_f^2}\left[2\hat{\mu}_x^{0f}\left(\Delta\hat{\mu}_x^{ff}\right)^2 - \left(\hat{\mu}_x^{0f}\right)^3\right] \qquad (8)$$

Using equations (7) and (8), the corresponding δ_{3P} becomes[66–68]

$$\delta_{3P}^{2SM} = 5\left(T_{xxx}^{2SM}\right)^2 \qquad (9)$$

All the results for 3PA are supplied in table 5 from which one can easily notice that similar to δ_{2P}, the gas phase δ_{3P} values are again smaller than the corresponding solvent-phase values. We have found that in both the gas phase and cyclohexane solvent, molecule C has the highest δ_{3P} value, whereas B has the least. In other two solvents, the highest value is for D and the lowest is again for B. It is also interesting to note that, similar to the 2PA process, the value of δ_{3P} is highest in CH_2Cl_2 solvent for all the systems, except B, where both the CH_2Cl_2 (5.59×10^8 a.u.) and C_2H_5OH (5.61×10^8 a.u.) values are very close to each other. In order to check the reliability of the 2SM results, we have computed, using response theory, different T_{ijk} terms and the overall δ_{3P} values for the first two molecules (i.e., A and B) in gas phase. These results are also supplied in table 5, which indicates that as per our anticipation (and similar to the 2PA results) the T_{xxx} tensor element is the highest contributing term for both the molecules. The values of T_{xxx} term (in 10^3 a.u. order) for A and B molecules, as calculated using response theory (and 2SM approach) are −10.75 (−9.11) and 8.91 (6.54), whereas that of overall δ_{3P} (in 10^8 a.u. order) are

Table 5. 3PA results as obtained using the 2SM approach and the response theory results.

	2SM results for T_{xxx} (in 10^3 a.u.) and δ_{3P} (in 10^8 a.u.) in different solvents			
System	Gas	Cyclohexane	CH_2Cl_2	C_2H_5OH
A	−9.60, 4.62	−17.43, 15.44	19.65, 19.92	19.16, 19.03
B	−9.11, 5.49	−13.86, 13.00	−14.82, 15.53	−14.46, 15.02
C	6.54, 1.92	−9.83, 4.32	11.26, 5.59	11.29, 5.61
D	−15.08, 12.41	−17.65, 16.91	−18.60, 18.91	−18.23, 18.22

Response theory results for T_{xxx} (in 10^3 a.u.) and δ_{3P} (in 10^8 a.u.) in gas phase

	T_{xxx}	T_{yyy}	T_{zzz}	T_{xxy}	T_{xxz}	T_{yyx}	T_{yyz}	T_{zzx}	T_{zzy}	T_{xyz}	δ_{3P}
A	−10.75	1.28	−0.04	2.09	0.35	−1.26	0.08	−0.06	−0.02	−0.15	7.42
B	8.91	0.69	−0.07	0.94	0.18	−0.84	0.03	−0.02	0.0	−0.02	3.71

7.42 (5.49) and 3.71 (1.92), respectively. These values are reasonably comparable with each other and hence it ensures the validity of the 2SM results. A close inspection of the x-component of both the μ^{0f} and $\Delta\mu^{ff}$ vectors indicate that the largest contribution of T_{xxx} tensor element and the highest value of δ_{3P} in CH_2Cl_2 solvent is because of the combined effect of the two vectors.

4. Conclusion

In conclusion, we have studied the solvent-dependent one-, two- and three-photon absorption processes in PRODAN (represented as D) and three newly synthesized chemosensors (denoted in this work as A, B and C) using both the response theory and the two-state model approach. We have found that compared to the other three molecules, D shows the highest one- and two-photon activity in both the gas as well as in different solvent phases. Regarding three-photon absorption, C shows the highest activity in gas phase and also in cyclohexane solvent, but D is again the most three-photon active system in other two solvents. In both the two- and three-photon absorption processes, the highest contributing tensor element (S_{xx} and T_{xxx}, respectively) corresponds to the charge-transfer between donor and acceptor moieties in these molecules. The highest contribution of S_{xx} tensor element is because of the larger value of x-component of μ^{0f}, whereas that of T_{xxx} is due to the combined effect of both the μ^{0f} and $\Delta\mu^{ff}$ vectors. For all the four molecules, the two- and three-photon activity is found to be the maximum in the solvent of intermediate polarity (here CH_2Cl_2). An inspection of different components of μ^{0f} and $\Delta\mu^{ff}$ vectors reveals that a combined effect of both of these vectors results in a high two- and three-photon activities of the systems in CH_2Cl_2 solvent. We have further noticed that the 2SM approach is quite successful in explaining the highest contribution of both the S_{xx} and T_{xxx} tensor elements in case of two- and three-photon absorption processes of these systems. Finally, we must mention that the future prospect of the present work includes the study of electronic non-adiabatic effects on the said properties. It would also be very interesting to study the solvent effect in full detail, including other solvents as well as both the equilibrium and non-equilibrium solvation techniques. In addition to these, one can also study these properties using higher-level computational methods such as coupled cluster.

Supplementary Information

The optimized coordinates of all the systems in gas phase and different solvents (cyclohexane, dichloromethane and ethanol) have been supplied in supplementary information file. The electronic supporting information can be seen at www.ias.ac.in/chemsci.

Acknowledgements

MA thanks the Council of Scientific and Industrial Research (CSIR) for the Senior Research Fellowship. MC thanks the Centre for Research in Nanoscience and Nanotechnology (CRNN) for the fellowship.

References

1. Weber G and Farris F J 1979 *Biochemistry* **18** 3075
2. MacGregor R B and Weber G 1981 *Ann. N.Y. Acad. Sci.* **366** 140
3. MacGregor R B and Weber G 1986 *Nature* **319** 70
4. Parusel A 1998 *J. Chem. Soc. Faraday Trans.* **94** 2923
5. Parusel A B J, Schneider F W and Köhler G J 1997 *Mol. Struct. (THEOCHEM).* **398** 341
6. Fernández-Suárez M and Ting A Y 2008 *Nature Rev. Mol. Cell Biol.* **9** 929
7. Kamal J K A, Zhao L and Zewail A H 2004 *Proc. Natl. Acad. Sc.* **101** 13411

8. Moreno F, Cortizo M and González-Jiménez J 1999 *Photochem-Photobiol.* **69** 8
9. Rottenberg H 1992 *Biochemisty.* **31** 9473
10. Parasassi T, Di Stefano M, Loiero M, Ravagnan G and Gratton E 1994 *Biophys. J.* **66** 120
11. Sengupta B, Guharay J and Sengupta P K 2000 *Spectrochim. Acta, Part A.* **56** 1433
12. Parasassi T, Giusti A M, Gratton E, Monoco E, Raimondi M, Ravagnan G and Sapora O 1994 *Int. J. Rad. Biol.* **65** 329
13. Massey J B, She H S and Pownall H J 1985 *Biochemistry.* **24** 6973
14. Sommer A, Paltauf F and Hermetter A 1990 *Biochemistry.* **29** 11134
15. Bondar O P and Rowe E S 1999 *Biophys. J.* **76** 956
16. Krasnowska E K, Bagatolli L A, Gratton E and Parasassi T 2001 *Biochim. Biophys. Acta.* **1511** 330
17. Wilson-Ashworth H A, Bahm Q, Erickson J, Shinkle A, Vu M P, Woodbury D and Bell J D 2006 *Biophys. J.* **91** 4091
18. Hutterer R and Hof M J 2001 *Fluorescence.* **11** 227
19. Sýkora J, Jurkiewicz P, Epand R M, Kraayenhof R, Langner M and Hof M 2005 *Chem. Phys. Lipids.* **135** 213
20. Benedetti E, Kocsis S L and Brummond K M 2012 *J. Am. Chem. Soc.* **134** 12418
21. Lobo B C and Abelt C J 2003 *J. Phys. Chem. A.* **107** 10938
22. Davis B N and Abelt C J 2005 *J. Phys. Chem. A.* **109** 1295
23. Mennucci B, Caricato M, Ingrosso F, Cappelli C, Cammi R, Tomasi J, Scalmani G and Frisch M 2008 *J. Phys. Chem. B.* **112** 414
24. Novaira M, Biasutti M A, Silber J J and Correa N M 2007 *J. Phys. Chem. B.* **111** 748
25. Adhikary R, Barnes C A and Petrich J W 2009 *J. Phys. Chem. B.* **113** 11999
26. Everett R K, Nguyen H A and Abelt C J 2010 *J. Phys. Chem. A.* **114** 4946
27. Cwiklik L, Aquino A J A, Vazdar M, Jurkiewicz P, Pittner J, Hof M and Lischka H 2011 *J. Phys. Chem. A.* **115** 11428
28. Olsen J and Jørgensen P 1985 *J. Chem. Phys.* **82** 3235
29. Linderberg J and Öhrn Y 1973 In *Propagators in Quantum Chemistry (New York: Academic)*.
30. Sałek P, Vahtras O, Helgaker T and Ågren H 2002 *J. Chem. Phys.* **117** 9630
31. Norman P, Jonsson D, Vahtras O and Ågren H 1996 *Chem. Phys.* **203** 23
32. Christiansen O, Jørgensen P and Hattig C 1998 *Int. J. Quantum Chem.* **68** 1
33. Cronstrand P, Luo Y and Ågren H 2002 *Chem. Phys. Lett.* **352** 262
34. Alam M M, Chattopadhyaya M and Chakrabarti S 2012 *Phys. Chem. Chem. Phys.* **14** 1156
35. Miertus S, Scrocco E and Tomasi J 1981 *Chem. Phys.* **55** 117
36. GAUSSIAN 09, revision C.01; Gaussian, Inc.: Wallingford, CT, (2010)
37. Mikkelsen K V, Ågren H, Jensen H J Aa and Helgaker T 1988 *J. Chem. Phys.* **89** 3086
38. Mikkelsen K V, Cesar A, Ågren H and Jensen H J Aa 1995 *J. Chem. Phys.* **103** 9010
39. DALTON, a molecular electronic structure program; release Dalton2011 (Rev. 0, July 2011). http://www.kjemi.uio.no/software/dalton/dalton.html (2011).
40. Mondol T, Reddy S R and Mahapatra S 2012 *J. Chem. Phys.* **137** 054311
41. Zgierski M Z, Fujiwara T and Lim E C 2005 *J. Chem. Phys.* **122** 144312
42. Studzinski H, Zhang S, Wang Y and Temps F 2008 *J. Chem. Phys.* **128** 164314
43. Mahapatra S 2009 *Acc. Chem. Res.* **42** 1004
44. Reddy V S, Ghanta S and Mahapatra S 2010 *Phys. Rev. Lett.* **104** 111102
45. Reddy S N and Mahapatra S 2013 *J. Phys. Chem. A.* **2013** 8737
46. Macak P, Luo Y, Norman P and Ågren H 2000 *J. Chem. Phys.* **113** 7055
47. Hilborn R C 1982 *Am. J. Phys.* **50** 982
48. Peach M J G, Benfield P, Helgaker T and Tozer D J 2008 *J. Chem. Phys.* **128** 044118
49. Chakrabarti S and Ruud K 2009 *J. Phys. Chem. A.* **113** 5485
50. Alam M M, Chattopadhyaya M and Chakrabarti S 2011 *Phys. Chem. Chem. Phys.* **13** 9285
51. Chattopadhyaya M, Alam M M and Chakrabarti S 2011 *J. Phys. Chem. A.* **115** 2607
52. Alam M M, Chattopadhyaya M, Chakrabarti S and Ruud K 2012 *J. Phys. Chem. Lett.* **3** 961
53. Alam M M, Chattopadhyaya M and Chakrabarti S 2012 *J. Phys. Chem. A.* **116** 8067
54. Alam M M, Chattopadhyaya M and Chakrabarti S 2012 *J. Phys. Chem. A.* **116** 11034
55. Mayer M G 1931 *Ann. Phys.* **9** 273
56. Kaiser W and Garrett C G B 1961 *Phys. Rev. Lett.* **7** 229
57. Abella I D 1962 *Phys. Rev. Lett.* **9** 453
58. Kawata S, Sun H B, Tanaka T and Takada K 1990 *Nature.* **412** 697
59. Albota M, Beljonne D, Brédas J L, Ehrlich J E, Fu J, Heikel A A, Hess S E, Kogej T, Levin M D, Marder S R, McCord-Maughon D, Perry J W, Rockel H, Rumi M, Subramaniam G, Webb W W, Wu X and Wu C 1998 *Science.* **281** 1653
60. Kogej T, Beljonne D, Meyers F, Perry J W, Mardar S R and Brédas J L 1998 *Chem. Phys. Lett.* **298** 1
61. Luo Y, Norman P, Macak P and Ågren H 2000 *J. Phys. Chem. A.* **104** 4718
62. Luo Y, Ågren H, Knuts S, Minaev B and Jørgensen P 1993 *Chem. Phys. Lett.* **209** 513
63. Luo Y, Ågren H, Knuts S and Jørgensen P 1993 *Chem. Phys. Lett.* **213** 357
64. Murugan N A, Kongsted J, Rinkevicius Z, Aidas K, Mikkelsen K V and Ågren H 2011 *Phys. Chem. Chem. Phys.* **13** 12506
65. Shen Y R 1984 In *The Principles of Nonlinear Optics (New York: Wiley) pp. 23–25*
66. Cronstrand P, Luo Y, Norman P and Ågren H 2003 *Chem. Phys. Letts.* **375** 233
67. Cronstrand P, Norman P, Luo Y and Ågren H 2004 *J. Chem. Phys.* **121** 2020
68. Cronstrand P, Jansik B, Jonsson D, Luo Y and Ågren H 2004 *J. Chem. Phys.* **121** 9239